Available Online

JSR Publications

J. Sci. Res. **16** (2), 527-535 (2024)

JOURNAL OF SCIENTIFIC RESEARCH

www.banglajol.info/index.php/JSR

Facile Room Temperature Deposition of ZnS Thin Films on Flexible Plastic Substrates via Nebulized Spray Method

A. Paul[1], J. C. John[2], J. Jose[3], V. J. Ambily[3], N. Joseph[1,3], S. Augustine[2,4], S. Thomas[4], T. Sebastian[1,4*]

[1]Department of Physics, Maharaja's College, Ernakulam, Kerala, India, 682 011

[2]Department of Physics, St. Thomas College, Pala, Kottayam, Kerala, India, 686 574

[3]Department of Physics, St. George's College, Aruvithura, Kottayam, Kerala, India, 686 122

[4]Department of Physics, Deva Matha College, Kuravilangad, Kottayam, Kerala, India, 686 633

Received 31 October 2023, accepted in final revised form 11 February 2024

Abstract

This study focuses on investigating a potential method for depositing zinc sulfide (ZnS), in thin film form at room temperature. A facile and effective approach was employed in this study, wherein a suspension of ZnS powder in methanol was applied onto flexible plastic substrates using a spray deposition method. Structural analysis of the resulting films revealed a broad X-ray diffraction peak along the (100) plane, indicating the presence of nanoscale crystallites. The band gap of the ZnS films was determined to be 3.78 eV. Furthermore, the films exhibited photo luminescence emission centered at a wavelength of 410 nm, which corresponds to the blue edge of the chromaticity diagram.

Keywords: Zinc sulfide; Nebulized spray method; Wurtzite phase; Optical properties; Photoluminescence; Chromaticity diagram.

doi: https://dx.doi.org/10.3329/jsr.v16i2.69566 J. Sci. Res. **16** (2), 527-535 (2024)

1. Introduction

Zinc sulfide (ZnS) is a II-VI compound semiconductor with a wide band gap of 3.7 eV, low absorption in visible and infra red (IR) spectral range and high refractive index [1]. It exists in two polymorphic forms- cubic sphalerite (β-ZnS) and hexagonal wurtzite (α-ZnS) [2]. Wurtzite phase is ideal for opto-electronic applications due to its large bandgap where as sphalerite is suitable in infrared transparent ceramic applications due to its optical isotropy [3].

ZnS thin films find applications in diverse fields such as sensors, flat panel displays, luminescent devices, photovoltaic devices etc [4-6]. ZnS films are reported to be deposited through physical and chemical methods such as vacuum evaporation, sputtering, chemical spray pyrolysis, chemical bath deposition, sol gel method, spin coating [7-10]. In spite of the variety of deposition techniques, room temperature deposition of ZnS thin

*Corresponding author: tina.sebastian@devamatha.ac.in

films remain challenging. Also, deposition of the synthesized ZnS powder in thin film form by simple methods such as doctor blading or spray coating is challenging due to the insolubility of ZnS in common solvents such as water or alcohol. A major advantage of room temperature deposition process is the prospect of the material to be coated on flexible substrates like plastic or polymers.

Existing methodologies employing the ZnS thin film deposition encounter challenges due to the necessity of high temperature conditions restricting their suitability for flexible or plastic substrates [11,12] In the realm of deposition processes, the allure of room temperature applications lies in their remarkable adaptability to coat materials onto flexible substrates, particularly plastics. This study embarks a novel route by presenting an innovative avenue for depositing ZnS thin films on plastic substrate at room temperature, employing the nebulized spray method. The distinctive appeal of this method lies not only in its capacity to preserve substrate flexibility but also in its originality as a cutting edge approach. Our primary objective is to explore the novel possibilities this technique offers. Unlike methods relying on sophisticated approaches like sputtering, our research showcases a method for effortlessly depositing ZnS thin films at room temperature on flexible substrates marking a noteworthy advancement [13,14]. The significance lies in the simplicity and practicality of achieving this deposition on plastic substrates, opening new possibilities for various applications [15]. Our exploration into the as prepared film's structural and optical properties mirrors the properties of ZnS thin films crafted through diverse techniques, weaving a narrative of consistency that strengthens the validity of our experimental outcomes.

2. Experimental Details

2.1. *Preparation of films*

Nebulized spray method was used for depositing films, where the precursor solution was converted to tiny droplets to form a fine spray. It was then sprayed on the substrate through the spray nozzle [16]. Thin films of ZnS were coated by spraying commercially available ZnS powder (Nice Chemicals, 98 % purity) dispersed in methanol on plastic substrates. Commercially available flexible plastic substrates were used for the deposition.

Initially the substrates were cleaned by soap solution, washed with distilled water, ultrasonically cleaned and dried. Mass of 0.1 g of ZnS powder was dispersed in 10 mL methanol and then sonicated for 15 min. It was then deposited using a nebulized sprayer on to cleaned flexible plastic substrates at room temperature and air dried. The spraytime was 10 min. Similar method of deposition has been previously reported for TiO_2 thin films [17]. This method of deposition is simple, cost effective, allows easier modifications in deposition parameters and does not require high temperature.

2.2. *Characterizations*

The properties of the ZnS thin films on flexible substrates were investigated by structural, morphological and optical characterization techniques. Structural characterization of the films were done using Rigaku Mini Flex 600 X-ray diffractometer with Cu-K_α irradiation (λ = 1.5406 A^o). Optical absorption studies were carried out using JASCO V-670 UV-Vis-NIR spectrophotometer. Surface analysis of the as-deposited films was carried out using scanning electron microscopy (TescanVega3). Photoluminescence studies were carried out using HORIBA Fluorolog-3 Phos spectrofluorometer.

3. Results and Discussion

3.1. *Structural studies*

X-ray diffraction technique (XRD) is a non destructive evaluation technique that helps to identify the crystal structure of the sample. Fig. 1a shows the XRD spectrum of the ZnS thin films.

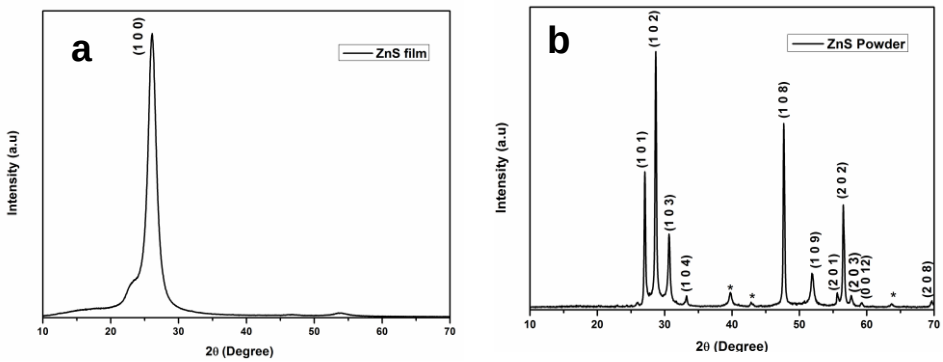

Fig. 1. XRD diffraction patterns of ZnS (a) thin film (b) powder.

X-ray diffractograms of ZnS thin films showed broad peak at 2θ= 26.08° that corresponds to the (100) plane. The pattern matched with ZnS with ICDD card No. 01-075-1547 which corresponded to ZnS with hexagonal structure. The wurtzite or hexagonal structure is the high temperature phase of ZnS. But, low temperature synthesis of hexagonal ZnS has also been reported [17,18]. In the present work, the commercial ZnS powder used for deposition also had hexagonal wurtzite structure which matched with the JCPDS card no. 892739. Fig. 1b shows the XRD pattern of ZnS powder in which the most intense peak at 2θ = 28.67° corresponding to (102) plane along with existence of other less intense peaks [(101), (103), (104), (108), (109), (201), (202), (203), (0012) and (208)]. Also there are some unidentified peaks which is denoted by * as shown in the

figure. These may be due to the impurities present in the powder sample. The multiple peaks present in the diffractogram of powder sample disappeared when the powder is deposited in the film form. Thus we could observe that dispersion in methanol and subsequent deposition in thin film form resulted in a drastic variation in structural properties.

The broadened diffraction peak confirms that the crystallite size is in nano regime. The broadening of XRD peak may be attributed to small crystallite size and lattice strain [19]. The crystallite size (D) of ZnS particles is calculated from the most intense peak using the Debye Scherrer formula [20].

$$D = \frac{k\lambda}{\beta \cos\theta} \quad (1)$$

Here, k = constant (0.9), β = full width at half maximum (in radians), λ = wavelength of light used (1.54 Å), θ = angle corresponding to the diffraction peak.The lattice strain ($\mathcal{E}$) of the samples can be calculated using the equation given below [21].

$$\mathcal{E} = \frac{\beta}{4\tan\theta} \quad (2)$$

Table 1 shows the crystallite size, lattice strain of both the ZnS powder and the thin film. From the table, it is observed that there is decrease in crystallite size and increase in the strain, when ZnS powder is made to the film form.

Table 1. Crystallite size and lattice strain of ZnS powder and film.

	Crystallite size(nm)	Lattice strain
ZnS powder	39.545	0.0027
ZnS film	18.418	0.4864

3.2. *Morphological studies*

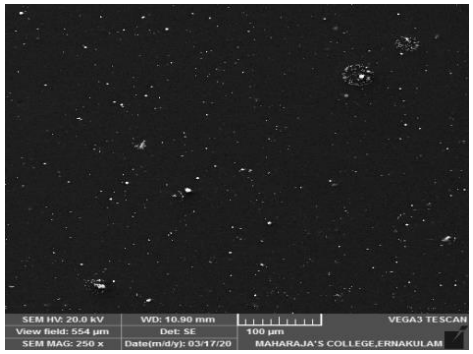

Fig. 2. SEM image of ZnS thin film.

The surface morphology of ZnS thin films deposited on flexible plastic substrates is shown in Fig. 2. The grains are not decipherable from the SEM image. Also, powdery deposits are seen to be distributed evenly over the surface of the film. But the ZnS film surface is observed to be free from cracks and pinholes. The substrate on which ZnS thin film deposited contributes to the morphology of the film [22]. The morphology of ZnS

thin films also depends upon different factors such as method of deposition, temperature etc. [23,24].

3.3. *Optical studies*

The optical properties of ZnS films were measured by absorption spectroscopy, transmission spectroscopy and photoluminescence (PL) studies. Fig. 3a shows the absorption spectra of ZnS thin films in the range of 200-800 nm. It is seen that there is increase in optical absorption in UV region.

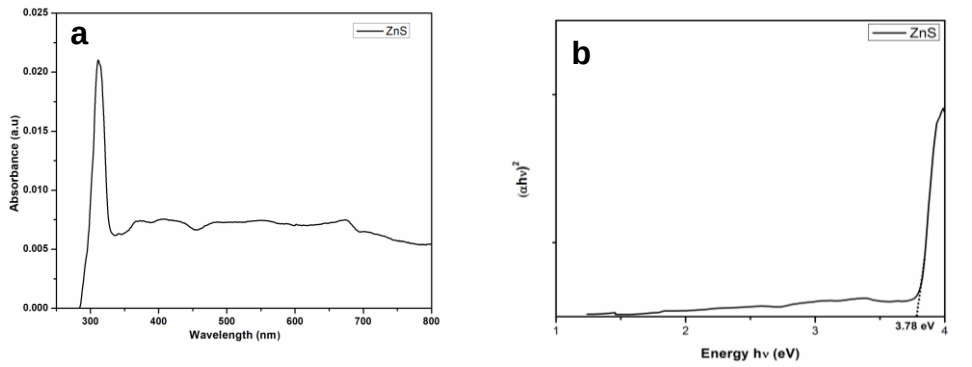

Fig. 3. (a) Absorption spectrum of ZnS thin film and (b) Tauc's plot to determine bandap of ZnS thin films.

Table 2. Comparison of bandgap with respect to the different precursors, spray techniques and temperature.

Precursors	Method of deposition	Temperature (°C)	Bandgap (eV)	References
$ZnCl_2$, Thiourea	Chemical Spray Pyrolysis	350	3.82	[16]
$ZnCl_2$, Thioacetamide	Chemical Spray Pyrolysis	310	3.64	[25]
$ZnCl_2$, Thiourea, Trisodium citrate	Chemical Spray Pyrolysis	300- 400	3.52- 3.72	[26]
$ZnCl_2$, Thiourea	Nebulized Spray Pyrolysis	400	3.56	[27]
$ZnCl_2$, Thiourea	Ultrasonic Spray	250- 400	3.88- 3.86	[28]
ZnS Powder	Nebulized Spray Technique	Room Temperature	3.78	[Present]

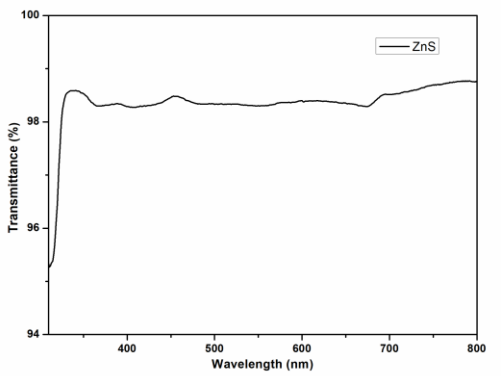

Fig. 4. Transmission spectra of ZnS thin films.

Fig. 4 shows the transmission spectrum of ZnS thin films. From the spectra, it was analyzed that ZnS thin films shows high transmittance in the visible range. The optical transmittance is found to be about 98 %. This opens up many applications for ZnS, especially as an antireflection coating material [29].Thus, transmission studies reveal the superior optical quality of the thin films deposited on the plastic substrates.

Photoluminescence is the emission of the light from the sample, when excited by light with energy greater than the optical band gap. The radiative recombination of the photoexcited carriers to the valence band may depend upon the defect states or impuritylevels present in the material [30]. Thus PL studies provide information about the band structure, impurity levels, path of carrier transport etc [31]. Fig. 5 represents the PL spectrum of ZnS thin films carried out at an excitation wavelength (λ_{ex}) of 311 nm and 340 nm respectively. The emission band obtained by light of wavelength 311 nm and 340 nm shows that both the PL peaks are centered at 410 nm. Here, it is noted that the emission band at 340 nm has much higher intensity. Thus the result shows that the emission spectrum of ZnS is obtained in the blue region of visible spectrum. The broad PL emission in blue region may be due to the transition from defect surface states to the valence band [31-33]. It has also been reported that reduction in particle size results shifting of PL emission more to the bluer region [33].

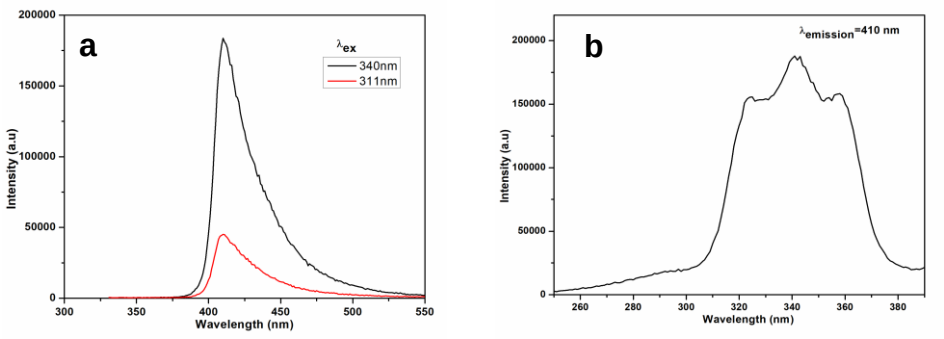

Fig. 5. (a) Emission spectra of ZnS thin films at 311 nm and 340 nm (b) Excitation spectra of ZnS thin films at 410 nm

The excitation spectrum of ZnS thin films is monitored at the emission wavelength (λ_{em}) at 410 nm and depicted in Fig. 5b. From the excitation spectra it is noted that, the intense peak is at 340 nm and two less intense peaks at 327 nm and 357 nm respectively.

Fig. 6 shows the Commission International d'Eclairage (CIE) diagrams of sprayed ZnS thin films and it confirms blue emission with CIE coordinates x= 0.15, y= 0.05. The percentage of color purity can be evaluated from the equation below [34].

$$color\ purity\ (\%) = \frac{\sqrt{(x_s - x_i)^2 + (y_s - y_i^2)}}{\sqrt{(x_d - x_i)^2 + (y_d - y_i)^2}} \times 100 \quad (3)$$

where (x_s,y_s) is the color coordinates of the sample. (x_i, y_i) is the illuminant point of the CIE diagram with the color coordinates. (x_d,y_d) is the color coordinates of the dominant wavelength.

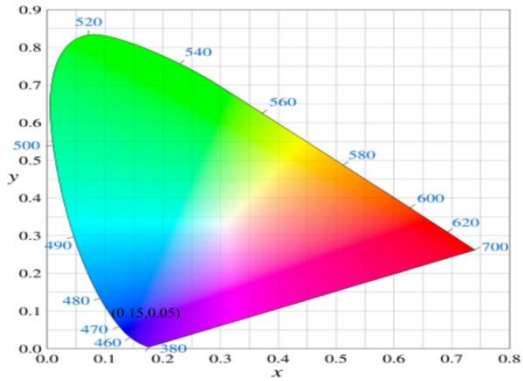

Fig. 6. CIE diagram of ZnS thin films.

From the calculation, it was found that the as-deposited ZnS thin films on plastic substrates exhibits color purity of about 94 %. The investigation of the PL emission spectra concluded the emission of blue light and the CIE diagram confirms this result

[35]. It reveals the excellent optical quality of the as deposited films. Therefore, the ZnS thin films deposited on plastic substrates could be an ideal blue light emitting material for optoelectronic applications [36].

4. Conclusion

In the present work, we have successfully deposited ZnS thin films on flexible plastic substrates at room temperature by nebulized spray method. Hexagonal wurtzite structure of the films and the resulting wide band gap makes it highly suitable for optoelectronic applications.The ZnS thin films deposited on flexible plastic substrates offers high transmittance of ~ 98 % in the visible spectral range. The pure blue emission from PL studies as evident from the position in CIE diagram also indicates the quality of ZnS films deposited by this process. Thus, spray deposition of ZnS thin films at room temperature is effectively achieved via this simple and cost effective route.

Acknowledgments

The authors are thankful to DST-FIST (SR/FST/College-101/ 2012) and the UGC (1904 – MRP/14-15/KLMG023/UGC – SWRO) for providing measurement facilities. This work is supported by Kerala State Council for Science, Technology and Environment (KSCSTE) and the authors acknowledge the financial support through student project (order no.00297/SPS 64/2019/KSCSTE).

References

1. K. Benyahia and A. Benhaya, M. S. Aida, J. Semicond. **36**, ID 103001 (2015). https://doi.org/10.1088/1674-4926/36/10/103001
2. Y. Li, W. Tan and Y. Wu, J. Eur. Ceram. Soc. **40**, 2130 (2020). https://doi.org/10.1016/j.jeurceramsoc.2019.12.045
3. S. I. Sadovnikov, Russ. Chem. Rev. **88**, 571 (2019). https://doi.org/10.1070/RCR4867
4. P. Roy, J. R. Ota, and S. K. Srivastava, Thin Solid Films **515**, 1912 (2006). https://doi.org/10.1016/j.tsf.2006.07.035
5. J. P. Borah and K. C. Sarma, Acta Phys. Pol. A **114**, 713 (2008). https://doi.org/10.12693/APhysPolA.114.713
6. J. P. Borah, J. Barman and K. C. Sarma, Chalcogenide Lett. **5**, 201 (2008).
7. M. B. Zaman, T. Chandel, K. Dehury, and P. Rajaram, AIP Conf. Proc. **100066** (2018).
8. B. Elidrissi, M. Addou, M. Regragui, A. Bougrine, A. Kachouane, and J. C. Bernède, Mater. Chem. Phys. **68**, 175 (2001). https://doi.org/10.1016/S0254-0584(00)00351-5
9. A. Goktas, F. Aslan, E. Yasar, and I. H. Mutlu, J. Mater. Sci. Mater. Electron. **23**, 1361 (2012). https://doi.org/10.1007/s10854-011-0599-z
10. T. K. Pathak, V. Kumar, L. P. Purohit, H. C. Swart, and R. E. Kroon, Phys. E Low-Dimensional Syst. Nanostruct. **84**, 530 (2016). https://doi.org/10.1016/j.physe.2016.06.020
11. A. Najim, B. Hartiti, H. Labrim, S. Fadili, M. Ertuğrul, and P. Thevenin, J. Mater. Sci. Mater. Electron. **33**, 15086 (2022). https://doi.org/10.1007/s10854-022-08428-x
12. A. A. Khadayeir, R. I. Jasim, S. H. Jumaah, N. F. Habubi, and S. S. Chiad, J. Phys. Conf. Ser. **1664,** ID 012009 (2020). https://doi.org/10.1088/1742-6596/1664/1/012009
13. M. S. Bashar, R. Matin, M. Sultana, A. Siddika, M. Rahaman, M. A. Gafur, and F. Ahmed, J.

Theor. Appl. Phys. **14**, 53 (2020). https://doi.org/10.1007/s40094-019-00361-5
14. A. M. Palve, Front. Mater. **6**, 1 (2019). https://doi.org/10.3389/fmats.2019.00046
15. Karimi, S. M. Mirkazemi, Y. Vahidshad, and J. Javadpour, Thin Solid Films **737**, ID 138929 (2021). https://doi.org/10.1016/j.tsf.2021.138929
16. T. A. Safeera, N. Johns, E. I. Anila, A. I. Martinez, P. V. Sreenivasan, R. Reshmi, M. Sudhanshu, and M. K. Jayaraj, J. Anal. Appl. Pyrolysis **115**, 96 (2015). https://doi.org/10.1016/j.jaap.2015.07.005
17. M. U. Bujnova, R. Todorovska, M. Milanova, R. Kralchevska, and D. Todorovsky, Appl. Surf. Sci. **256**, 830 (2009). https://doi.org/10.1016/j.apsusc.2009.08.069
18. Y. Zhao, Y. Zhang, H. Zhu, G. C. Hadjipanayis, and J. Q. Xiao, J. Am. Chem. Soc. **126**, 6874 (2004). https://doi.org/10.1021/ja048650g
19. P. Bindu and S. Thomas, J. Theor. Appl. Phys. **8**, 123 (2014). https://doi.org/10.1007/s40094-014-0141-9
20. C. S. Tiwary, S. Saha, P. Kumbhakar, and K. Chattopadhyay, Cryst. Growth Des. **14**, 4240 (2014). https://doi.org/10.1021/cg500657e
21. N. Bouguila, D. Bchiri, M. Kraini, A. Timoumi, I. Halidou, K. Khirouni, and S. Alaya, J. Mater. Sci.: Mater. Electron. **26**, 9845 (2015). doi.org/10.1007/s10854-015-3659-y
22. C. M. Gõmez-Gutiérrez, P. A. Luque, A. Castro-Beltran, A. R. Vilchis-Nestor, E. Lugo-Medina, A. Carrillo-Castillo, M. A. Quevedo-Lopez, and A. Olivas, J. Scanning Microscopy **37**, 389 (2015). https://doi.org/10.1002/sca.21227
23. L. Li Hou and F. Gao, Mater. Lett. **65**, 500 (2011). https://doi.org/10.1016/j.matlet.2010.10.061
24. F. Göde, Physica B: Condensed Matter **406**, 1653 (2011). https://doi.org/10.1016/j.physb.2010.12.033
25. X. Zeng, S. S. Pramana, S. K. Batabyal, S. G. Mhaisalkar, X. Chen, and K. B. Jinesh, Phys. Chem. Chem. Phys. **15**, 6763 (2013). https://doi.org/10.1039/c3cp43470b
26. P. O. Offor, B. A. Okorie, C. D. Lokhande, P. S. Patil, F. I. Ezema, A. D. Omah, V. S. Aigbodion, B. A. Ezekoye, and I. C. Ezema, Int. J. Adv. Manuf. Technol. **95**, 1849 (2018). https://doi.org/10.1007/s00170-017-1326-6
27. C. Sabitha, I. H. Joe, K. D. A. Kumar, and S. Valanarasu, Opt. Quantum Electron. **50**, 1 (2018). https://doi.org/10.1007/s11082-018-1418-z
28. W. Daranfed, M. S. Aida, A. Hafdallah, and H. Lekiket, Thin Solid Films **518**, 1082 (2009). https://doi.org/10.1016/j.tsf.2009.03.227
29. E. Márquez, E. R. Shaabanand, and A. M. Abousehly, Int. J. New. Hor. Phys. **1**, 17 (2014).
30. K. N. Shinde, S. J. Dhoble**,** H. C. Swart**,** and K. Park, Springer Series Mater. Sci. **174**, (Springer-Verlag Berlin Heidelberg, 2012). https://doi.org/10.1007/978-3-642-34312-4
31. R. Keshav and M. MG, Mater. Res. Bull. **105**, 360 (2018). https://doi.org/10.1016/j.materresbull.2018.05.018
32. T. A. Safeera, N. Johns, and E. I Anila, Opt. Mat. **58**, 32 (2016) https://doi.org/10.1016/j.optmat.2016.03.050
33. R. K. Chandrakar, R. N. Baghel, V. K. Chandra, and B. P. Chandra, Superlattice Microst. **84**, 132 (2015). https://doi.org/10.1016/j.spmi.2015.04.023
34. D. Prakashbabu, H. B. Ramalingam, R. Hari Krishna, B. M. Nagabhushana, R. Chandramohan, C. Shivakumara, J. Thirumalai, and T. Thomas, Phys. Chem. Chem. Phys. **18**, 29447 (2016). https://doi.org/10.1039/C6CP04633A
35. E. I. Anila, T. A Safeera, and R. Reshmi, J. Fluoresc. **25**, 227 (2015). https://doi.org/10.1007/s10895-015-1515-3
36. Z. Li, B. Liu, X. Li, S. Yu, L. Wang, Y. Hou, Y. Zou, M. Yao, Q. Li, B. Zou, T. Cui, G. Zou, G. Wang, and Y. Liu, Nanotechnology **18**, ID 255602 (2007). https://doi.org/10.1088/0957-4484/18/25/255602